Available online at www.sciencedirect.com
SCIENCE DIRECT
ELSEVIER
International Journal of Pharmaceutics 320 (2006) 165–170
INTERNATIONAL JOURNAL OF PHARMACEUTICS
www.elsevier.com/locate/ijpharm

Pharmaceutical Nanotechnology

Lipid nanocapsule size analysis by hydrodynamic chromatography and photon correlation spectroscopy

Betül Arıca Yegin [a], Alf Lamprecht [b,*]

[a] *Department of Pharmaceutical Technology, Faculty of Pharmacy, Hacettepe University, 06100 Sıhhiye-Ankara, Turkey*
[b] *Laboratory of Pharmaceutical Engineering, Faculty of Medicine and Pharmacy, University of Franche-Comté, 25000 Besançon, France*

Received 6 February 2006; received in revised form 22 April 2006; accepted 24 April 2006
Available online 30 April 2006

Abstract

Particle size and the size distribution are known to be important factors in the overall behavior of nanoparticulate drug delivery systems and an exact determination of these parameters is highly important. Several techniques are applied in the size determination of nanoparticulates, particularly dynamic light scattering. Also other methods have been proposed, among them hydrodynamic chromatography (HDC). In order to characterize a HDC method for nanosized carriers, differently sized lipid nanocapsules having a diameter of 25–100 nm were analyzed and results were compared with measurements from photon correlation spectroscopy (PCS) and atomic force microscopy. Results from atomic force microscopy studies were generally not in line with determinations from the other techniques due to a particle shape loss by the drying step. PCS and HDC led to comparable results in simple size determination of lipid nanocapsules. However, slight differences were found during the characterization of more complex samples. HDC was able to detect micelles as a byproduct of nanocapsule preparation while in PCS the sample dilution turned micelles undetectable. HDC analysis was able to characterize mixed samples of particle batches differing in their average size similar to PCS. HDC was found to be an excellent tool for the determination of size and average size distribution of lipid nanocapsules.

Keywords: Nanoparticles; Particle size; Size distribution; Photon correlation spectroscopy; Hydrodynamic chromatography

1. Introduction

Modern drug carrier systems play an important role in controlled delivery of the pharmacological agent to its target at a therapeutically optimal rate and dose. Among various colloidal drug delivery systems nanoparticles represent a promising approach to this aim (Kreuter, 1994; Takeuchi et al., 2001; Brigger et al., 2002; Panyam and Labhasetwar, 2003; Bala et al., 2004). These carriers are of interest due to the small particle size, which allows a drug transport across biological membranes or specific targeting by a possible surface modification (Bourel et al., 1988; Ponchel and Irache, 1998; Kreuter, 2001). For the nanoencapsulation, many different techniques have been developed. Polymeric carriers were prepared by either polymerization methods or the use of preformed polymers (Kreuter, 1994). Other strategies have been proposed to design lipid nanoparticles for drug delivery (Müller et al., 2000; Bummer, 2004).

The exact knowledge of size and size distribution is essential for such nanoparticulate drug delivery systems, since these parameters can significantly modify physicochemical as well as biopharmaceutical behavior, for example changing drug release kinetics or transport phenomena across biological barriers (Hillyer and Albrecht, 2001; Lamprecht et al., 2002).

Nowadays, photon correlation spectroscopy (PCS) is the standard method for the determination of particle diameter and size distribution of nanoparticles. This method is also referred to as dynamic light scattering and quasi-elastic light scattering. The pace of the movement of particles in water is inversely proportional to particle size, and can be detected by analyzing the time dependency of the light intensity fluctuations scattered from the particles when they are illuminated with a laser beam. In dynamic light scattering one measures the time dependence of the light scattered from a very small region of solution, over a time range from 10th of a microsecond to milliseconds. These fluctuations in the intensity of the scattered light are related to the rate of diffusion of particles in and out of the region being

* Corresponding author at: Place Saint Jacques, 25000 Besançon, France. Tel.: +33 3 81 66 55 48; fax: +33 3 81 66 52 90.
E-mail address: alf.lamprecht@univ-fcomte.fr (A. Lamprecht).

0378-5173/$ – see front matter © 2006 Elsevier B.V. All rights reserved.
doi:10.1016/j.ijpharm.2006.04.014

studied (Brownian motion), and the data can be analyzed to directly give the diffusion coefficients of the particles doing the scattering. Traditionally, rather than presenting the data in terms of diffusion coefficients, the data are processed to give the "size" of the particles (radius or diameter) which is based on theoretical relationship between the Brownian motion and size of spherical particles.

Besides, field flow fractionation (FFF) has been used in several projects to determine the mass of proteins and size of colloidal carriers, including liposomes, injectable emulsions, and particles (Caldwell et al., 1972; Giddings, 1993; Jores et al., 2004; Fraunhofer et al., 2004; Andersson et al., 2005). This technique showed certain advantages over common size determination procedures, since a separation precedes the detection of the sample or sample components. Due to their low density, particles smaller than 100 nm were excluded from this type of size determination. However, gold nanoparticles for the application in protein labeling were mentioned in literature to be successfully analyzed for their size distribution by sedimentation field-flow fractionation (Anger et al., 1999).

The hydrodynamic chromatography (HDC) separation relies on the size-dependent exclusion from the wall in a channel in which a pressure-driven flow is applied. The corresponding parabolic flow profile results in a larger velocity for larger analytes, since they will on the average spend more time in the faster flowing regions of the channel. Classically, HDC is performed in columns packed with nonporous particles giving a relatively small efficiency especially for small packing particle sizes (Venema et al., 1996). In narrow conduits (effective size <1 μm) with a laminar flow, larger molecules or particles (size range from 0.002 to 0.2 of the conduit size) are transported faster than smaller ones as they cannot fully access slow-flow regions near the conduit walls (Small et al., 1976; Tijssen et al., 1986). In HDC, this is used for analytical separation in applications similar to traditional size exclusion chromatography. The separation effect occurs in packed columns, open microcapillaries or flat microchannels.

The aim of the study was to determine exemplarily the potential of the HDC method for the size analysis of nanoparticulate drug delivery systems. Different batches of lipid nanocapsules (LNC) were prepared by a phase inversion process in a size range of 25–100 nm (Lamprecht et al., 2002). Due to the very small size and the simple preparation procedure allowing the fabrication of particles of different sizes, these LNC were used in this study as model nanocarriers with a certain softness. Results from HDC analyses on various particle batches and their respective mixtures were compared with measurements from PCS and atomic force microscopy, which provided additional information as an imaging approach.

2. Materials and methods

2.1. Materials

Medium-chain triglycerides (Labrafac® CC) were kindly provided by Gattefossé (Saint-Priest, France). Soybean lecithin (Lipoid® S75-3) and polyethylene glycol-660 hydroxystearate (PEG–HS, Solutol® HS15) were kind gifts from Lipoid GmbH (Ludwigshafen, Germany) and BASF AG (Ludwigshafen, Germany), respectively. All other chemical reagents were obtained from Sigma (Steinheim, Germany) and Fisher Scientific (Elancourt, France) and were of analytical grade.

Table 1
Composition of the components for the nanocapsule preparation for a total initial mass of 5.0 g

	Water (%)	Oil (%)[a]	Surfactant (%)[b]
LNC25	65	25	10
LNC50	61.25	21.25	17.5
LNC100	42.5	17.5	40

[a] Labrafac® CC.
[b] Solutol® HS15.

2.2. Preparation of LNC

Different LNC formulations at nominal sizes of 25, 50, and 100 nm were prepared by a phase inversion processing recently reported in literature (Heurtault et al., 2002). The detailed composition is given in Table 1. Briefly, The oil phase was mixed with the appropriate amounts of surfactant (PEG–HS), lecithin, sodium chloride, and distilled water and heated under magnetic stirring up to 85 °C (until a distinct drop of conductivity occurs) ensuring that the phase inversion temperature is passed. The cooling step was then performed until an exact temperature of 55 °C was reached, again, completely passing the phase inversion zone. This cycle was repeated another two times before adding 5 ml of distilled cold water at 2 °C. The formulation was stirred for another 10 min before further use.

2.3. Particle size analysis of LNC

LNC suspensions were diluted 1:100 (or higher) for PCS measurements. For the analysis of mixtures, all samples were composed by mixing 1 ml of each differently sized LNC batch and either applied pure (HDC) or in a 1:500 dilutions to the analysis (PCS). To prepare samples for the mixture, differently sized LNC were dialyzed (pore size: 100.000 Da) against distilled water until no PEG–HS was detected in the acceptor phase in order to ensure a minimum of free surfactant in all batches.

2.3.1. Hydrodynamic chromatography (HDC)

A commercialized PL-PSDA Particle Size Distribution Analyser (Polymer Laboratories Ltd., Church Stretton, UK) was used for the size distribution analysis. The PL-PSDA was operated on the principle of packed column HDC, a technique for separating particles based on their size, eluting in the order largest to smallest. The sample flows through the cartridge, which contains a packed bed of non-porous particles. Larger particles are less mobile and tend to remain in the central region of flow in the capillary, while smaller particles tend to migrate to the wall. The fractionation is therefore based on the variation of retention time for differently sized particles. A water-based eluent was continuously pumped through the system at a constant flow rate

of 1.70 ml/min, the pressure was varying between 8.38 and 8.46 and the analysis time was 600 s. The UV detector response is used to calculate the concentration of particles of different size present in the sample. Samples were analyzed against standards of particles of nominal size of 19 and 50 nm, respectively.

Two milliliter of each undiluted LNC sample under investigation were introduced into the system via a two position, electrically actuated valve, so as the eluent flow is not interrupted.

2.3.2. Photon correlation spectroscopy

The LNC were analyzed for their size and size distribution by PCS in order to allow the comparison of results with HDC. The average volume diameters and the polydispersity index were determined by a Malvern Autosizer® 4700 (Malvern Instruments S.A., Worcestershire, UK) fitted with a 488 nm laser beam at a fixed angle (90°) at 25 °C. All batches were diluted with distilled water prior to the analysis and filtered through a 0.2 μm Millipore Sartorius filter (Millipore, France).

2.3.3. LNC imaging by atomic force microscopy (AFM)

The characterization of LNC was performed with a commercial AFM (Autoprobe cp®, Parc Scientific Instruments, Sunnyvale, USA) equipped with a 2 μm cantilever and a monocrystalline silicium tip Ultralever UL020 (Park Scientific Instrument, Geneva, Switzerland). The linear scanning rate was 1 Hz. The AFM was only used in the contact mode and the force was adjusted to 10 nN. LNC samples were diluted 1:200 before being placed on a mica plate surface by dropping 20 μl of the suspension onto the surface and removing the water under slightly reduced pressure overnight.

3. Results and discussion

In AFM studies, after spreading of the LNC suspension on a mica plate, the LNC flattened due to the drying step during sample preparation. Subsequently, all formulations appeared in a disk-like shape. Fig. 1 represents LNC of the different batches of LNC prepared as described in Table 1. LNC appeared spherical but the size was distinctly higher than that determined by HDC and PCS. LNC did not fuse during the sample preparation in contrast to what was reported from AFM images of liposomes (Solletti et al., 1996; Thomson et al., 2000). By scanning the LNC surface with the tip in the contact mode, slight deformations of the capsule surface can be observed. Also in earlier AFM studies of solid lipid nanoparticles such observation were made, that particles flattened during the AFM sample preparation which led to a higher diameter on the AFM images than measured by PCS (zur Mühlen et al., 1996). Although AFM images gave an overall impression of the relative changes in particle sizes, this technique was not applicable for the exact particle size determination of this rather flexible type of nanocarrier.

The particle size distribution of LNC measured by PCS was in the range of 25–100 nm (Fig. 2). As reported in Table 2, LNC batches had a low polydispersity index (0.058–0.091) and showed a monomodal particle size distribution. The size determination was performed at high dilutions (1:100 and higher)

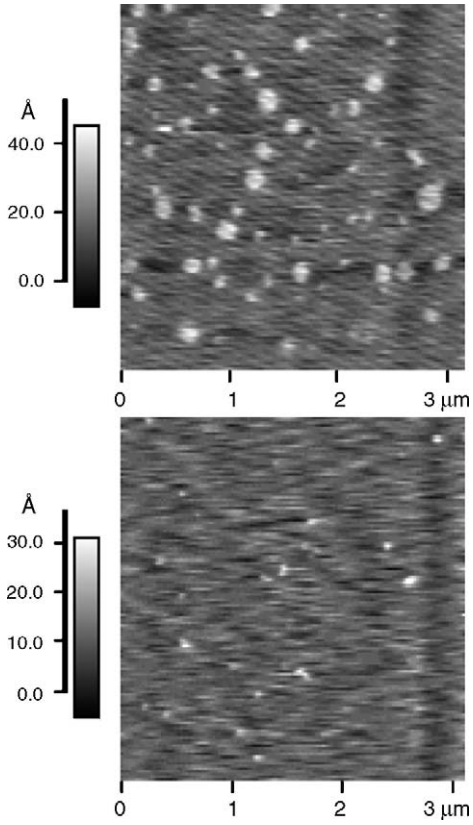

Fig. 1. Atomic force microscopic image of LNC of the different sizes: LNC100 (upper) and LNC25 (lower).

whereas it was found that smaller LNC required a distinct higher concentration for an exact measurement. Moreover, it has to be kept in mind that some of the PCS instruments supply the calculation of diameter by the Mie theory. However, when the particle size decreases to $d \leq \lambda/10$ (where λ is the wavelength of light) the approximation of Rayleigh scattering is the most appropriate. In

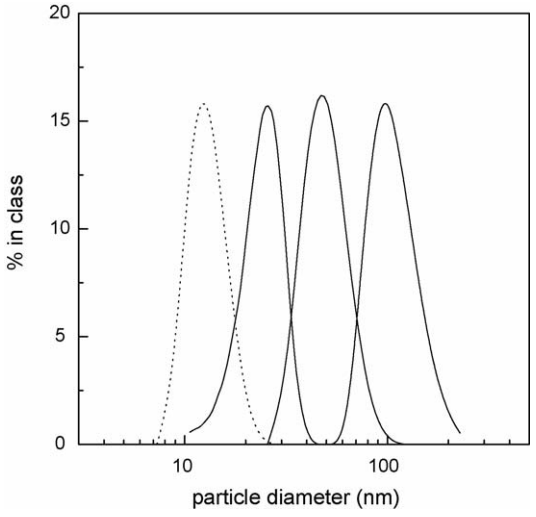

Fig. 2. Size distribution of the different formulations reported from Table 2, representing LNC (straight lines, LNC25: left; LNC50: middle; LNC100: right) compared to PEG–HS micelles (dotted line). All curves show representative measurements.

Table 2
Particle size and polydispersity indices of different LNC batches (PCS samples: 1:100 diluted, HDC samples: undiluted)

	PCS		HDC	
	Mean particle size (nm)	Polydispersity index	Mean particle size (nm)	Coefficient of variances (%)
LNC25	26.6 ± 3.3	0.091 ± 0.025	22.5 ± 3.1	10.3
LNC50	50.5 ± 4.9	0.058 ± 0.034	49.5 ± 3.7	30.7
LNC100	97.5 ± 6.8	0.070 ± 0.040	101.8 ± 6.2	36.9

Data are shown as mean ± S.D. ($n = 3$).

times where one of the aims is the decrease of nanocarriers down towards a few nanometers to meet virus-like sizes this must be taken into account.

When LNC were analyzed by HDC, the three different batches were applied separately either pure or in a 1:100 dilution. In general, no significant influence by the dilution step was observed concerning the particle diameter. It also has to be mentioned that a relatively high coefficient of variation is observed with HDC when analyzing the differently sized batches compared to results obtained with polymeric carriers (Chmela et al., 2002; Blom et al., 2003). This effect remained unclear, could be however related to a certain elasticity of LNC leading to an increased variation of the determined particle diameter. Further studies seemed to be necessary to elucidate this effect. While with diluted LNC25 samples, the size and size distribution in HDC was equivalent to results obtained with PCS (Fig. 3A), undiluted samples led to a surprising additional observation, which was not found in PCS measurements. LNC25 samples exhibited a second peak in the size distribution (Fig. 3B). Based on prior determinations, this peak represents a diameter similar to that of micelles and might therefore suggest the presence of micelles in the preparation, since a second population might be excluded by the PCS measurements. In PCS studies, the presence of such micelles might be not found probably due to their too low concentration in the diluted sample. Another possibility is that the dilution steps in PCS sample preparation lowers the free surfactant concentration that much, that it passes below the critical micelle concentration and micellar structures were destroyed. It should be however mentioned that recent ameliorations in this technique allow the analysis of concentrated dispersions circumventing this drawback.

Generally, it could be important to determine such incidences on the formation of micelles for possible further conclusions about the behavior of the drug loaded carrier system. If micelles coexist beside the formed LNC, they can distinctly affect parameters such as the biodistribution or the drug release since they theoretically represent an independently acting drug delivery system which shows the example of mixed micelles for drug delivery (Yokoyama et al., 1990; Yokoyama et al., 1991). As described in previous works, a dislocation of the surfactant can be observed with the time from the nanoparticle surface in dependency of carrier and surfactant type (Lamprecht et al., 2002; Lamprecht and Benoit, 2006). Since various surfactant types are applied in the development of nanoparticles, e.g. polysorbate, sodium cholate, etc., a hypothetic influence by coexisting micelles might reach a broad field of nanoencapsulation techniques and applications. In consequence, those coexisting micelles risk altering the drug delivery properties and the biodistribution of the developed systems distinctly. Thus, particle size analyses with HDC allowed elucidating an additional aspect in nanoparticle design, which has hardly described in literature until now.

A second aspect of comparison of PCS and HDC methods was the ability to differentiate particle size populations in mixed samples. While the determinations of PCS were rather diffi-

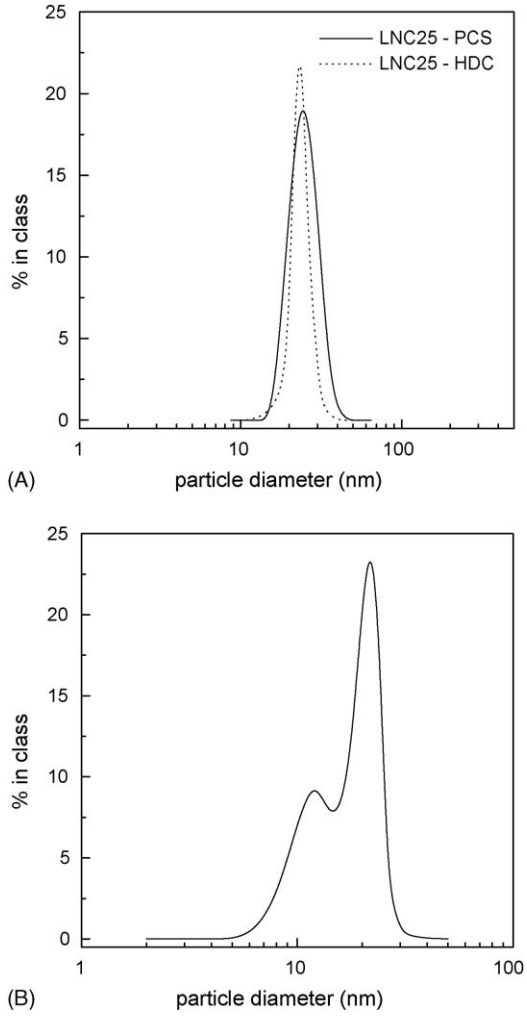

Fig. 3. Size distribution of LNC25 as diluted sample (1:100 dilution) analyzed with PCS and HDC (A) compared to the particle size distribution obtained for pure LNC25 with HDC (B). A and B display representative measurements.

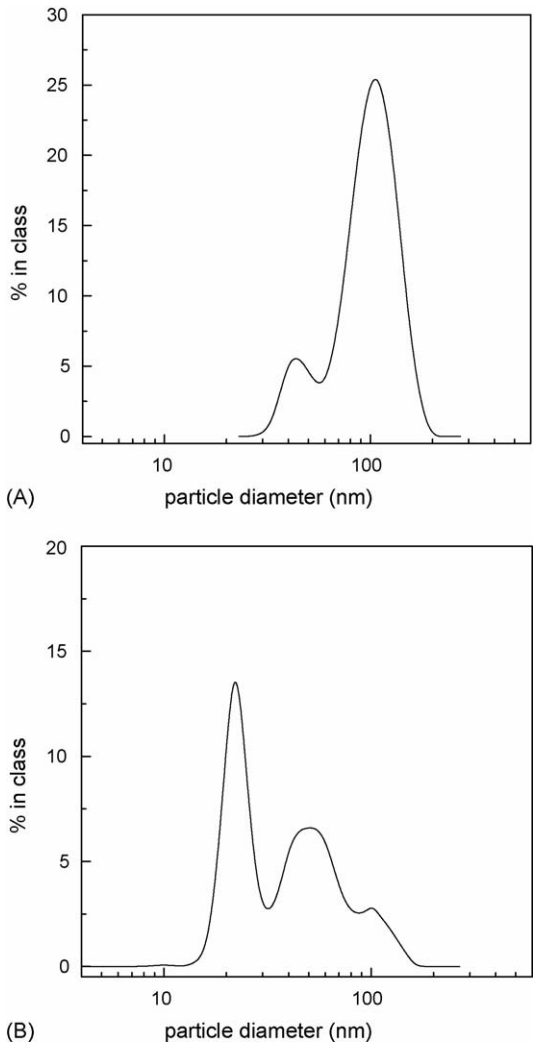

Fig. 4. Size distribution analysis of a mixture of equivalent volumetric quota of the three formulations (see Table 2) as diluted sample analyzed with PCS (A) compared to the distribution obtained for the same but pure mixture measured by HDC (B). A and B display representative measurements.

cult to interprete for this composition resulting in the absence of a LNC25 signal (Fig. 4A), results with HDC were slightly better and subsequently three peaks were found in the analysis which fitted well into the determined size of that was obtained by separated measurements (Fig. 4B). The signal was distinctly dependent on the number of LNC in the mixture, where highest signal was found for LNC25.

4. Conclusions

While AFM imaging can be considered as insufficient for the particle size of such carriers, PCS and HDC were comparable in terms of simple size determination. Besides, HDC allowed the discovery of micellar systems existing beside the nanocapsules in the suspension. This method of particle analysis permitted to determine size distribution of mixes of different LNC batches where PCS analyses were less accurate. In consequence, non-fractionation techniques appear to be less appropriate for the analysis of multi-modal samples and samples with broad particle size distributions due to the low resolution of the method.

References

Andersson, M., Fromell, K., Gullberg, E., Artursson, P., Caldwell, K.D., 2005. Characterization of surface-modified nanoparticles for in vivo biointeraction. A sedimentation field flow fractionation study. Anal. Chem. 77, 5488–5493.

Anger, S., Caldwell, K., Niehus, H., Müller, R.H., 1999. High resolution size determination of 20 nm colloidal gold particles by SedFFF. Pharm. Res. 16, 1743–1747.

Bala, I., Hariharan, S., Kumar, M.N., 2004. PLGA nanoparticles in drug delivery: the state of the art. Crit. Rev. Ther. Drug Carrier Syst. 21, 387–422.

Blom, M.T., Chmela, E., Oosterbroek, R.E., Tijssen, R., van den Berg, A., 2003. On-chip hydrodynamic chromatography separation and detection of nanoparticles and biomolecules. Anal. Chem. 75, 6761–6768.

Bourel, D., Rolland, A., Le Verge, R., Genetet, B., 1988. A new immunoreagent for cell labeling CD3 monoclonal antibody covalently coupled to fluorescent polymethacrylic nanoparticles. J. Immunol. Methods 106, 161–167.

Brigger, I., Dubernet, C., Couvreur, P., 2002. Nanoparticles in cancer therapy and diagnosis. Adv. Drug Deliv. Rev. 54, 631–651.

Bummer, P.M., 2004. Physical chemical considerations of lipid-based oral drug delivery—solid lipid nanoparticles. Crit. Rev. Ther. Drug Carrier Syst. 21, 1–20.

Caldwell, K.D., Kesner, L.F., Myers, M.N., Giddings, J.C., 1972. Electrical field-flow fractionation of proteins. Science 176, 296–298.

Chmela, E., Tijssen, R., Blom, M.T., Gardeniers, H.J., van den Berg, A., 2002. A chip system for size separation of macromolecules and particles by hydrodynamic chromatography. Anal. Chem. 74, 3470–3475.

Fraunhofer, W., Winter, G., Coester, C., 2004. Asymmetrical flow field-flow fractionation and multiangle light scattering for analysis of gelatin nanoparticle drug carrier systems. Anal. Chem. 76, 1909–1920.

Giddings, J.C., 1993. Field-flow fractionation: analysis of macromolecular, colloidal, and particulate materials. Science 260, 1456–1465.

Heurtault, B., Saulnier, P., Pech, B., Proust, J.E., Benoit, J.P., 2002. A novel phase inversion-based process for the preparation of lipid nanocarriers. Pharm. Res. 19, 875–880.

Hillyer, J.F., Albrecht, R.M., 2001. Gastrointestinal persorption and tissue distribution of differently sized colloidal gold nanoparticles. J. Pharm. Sci. 90, 1927–1936.

Jores, K., Mehnert, W., Drechsler, M., Bunjes, H., Johann, C., Mäder, K., 2004. Investigations on the structure of solid lipid nanoparticles (SLN) and oil-loaded solid lipid nanoparticles by photon correlation spectroscopy, field-flow fractionation and transmission electron microscopy. J. Control. Release 95, 217–227.

Kreuter, J., 1994. Colloidal Drug Delivery Systems. Drugs and the Pharmaceutical Sciences, vol. 66. Marcel Dekker, New York.

Kreuter, J., 2001. Nanoparticulate systems for brain delivery of drugs. Adv. Drug Deliv. Rev. 47, 65–81.

Lamprecht, A., Benoit, J.P., 2006. Etoposide nanocarriers suppress glioma cell growth by intracellular drug delivery and simultaneous P-glycoprotein inhibition. J. Control. Release 112, 208–213.

Lamprecht, A., Bouligand, Y., Benoit, J.P., 2002. New lipid nanocapsules exhibit sustained release properties for amiodarone. J. Control. Release 84, 59–68.

Müller, R.H., Mäder, K., Gohla, S., 2000. Solid lipid nanoparticles (SLN) for controlled drug delivery—a review of the state of the art. Eur. J. Pharm. Biopharm. 50, 161–177.

Panyam, J., Labhasetwar, V., 2003. Biodegradable nanoparticles for drug and gene delivery to cells and tissue. Adv. Drug Deliv. Rev. 55, 329–347.

Ponchel, G., Irache, J., 1998. Specific and non-specific bioadhesive particulate systems for oral delivery to the gastrointestinal tract. Adv. Drug Deliv. Rev. 34, 191–219.

Small, H., Saunders, F.L., Solc, J., 1976. Hydrodynamic chromatography a new approach to particle size analysis. Adv. Colloid Interface Sci. 6, 237–266.

Solletti, J.M., Botreau, M., Sommer, F., Brunat, W.L., Kasas, S., Duc, T.M., Celio, M.R., 1996. Elaboration and characterization of phospholipid Langmuir-Blodgett films. Langmuir 12, 5379–5386.

Takeuchi, H., Yamamoto, H., Kawashima, Y., 2001. Mucoadhesive nanoparticulate systems for peptide drug delivery. Adv. Drug Deliv. Rev. 47, 39–54.

Thomson, N.H., Collin, I., Davies, M.C., Palin, K., Parkins, D., Roberts, C.J., Tendler, S.J.B., Williams, P.M., 2000. Atomic force microscopy of cationic liposomes. Langmuir 16, 4813–4818.

Tijssen, R., Bos, J., van Kreveld, M.E., 1986. Hydrodynamic chromatography of macromolecules in open microcapillary tubes. Anal. Chem. 58, 3036–3044.

Venema, E., Kraak, J.C., Poppe, H., Tijssen, R., 1996. Packed-column hydrodynamic chromatography using 1-μm non-porous silica particles. J. Chromatogr. A 740, 159–167.

Yokoyama, M., Miyauchi, M., Yamada, N., Okano, T., Sakurai, Y., Kataoka, K., Inoue, S., 1990. Characterization and anticancer activity of the micelle-forming polymeric anticancer drug adriamycin-conjugated poly(ethylene glycol)-poly(aspartic acid) block copolymer. Cancer Res. 50, 1693–1700.

Yokoyama, M., Okano, T., Sakurai, Y., Ekimoto, H., Shibazaki, C., Kataoka, K., 1991. Toxicity and antitumor activity against solid tumors of micelle-forming polymeric anticancer drug and its extremely long circulation in blood. Cancer Res. 51, 3229–3236.

zur Mühlen, A., zur Mühlen, E., Niehus, H., Mehnert, W., 1996. Atomic force microscopy studies of solid lipid nanoparticles. Pharm. Res. 13, 1411–1416.